istics of the Colloid Core Reactor," AIAA Paper 72-1094, New Orleans, La., 1972.

[6] "Space Shuttle Baseline Recommendations for Payloads," June 27, 1972, NASA.

[7] Durham, F. P. and Kirk, W. L., "The Design of a Nuclear Rocket Engine for Unmanned Missions to the Outer Planets," AIAA Paper 72-1090, New Orleans, La., 1972.

[8] Dugan, D. W., "Comparative Performance of Nuclear and Cryogenic Chemical Space Propulsion Systems," TM X-2352, 1971, NASA.

[9] Finke, R. G. and Oliver R. C., "Comparison of Chemical and Nuclear Propulsion for Lunar and Cislunar Transportation Systems," Paper P-687, 1970, Inst. for Defense Analysis, Arlington, Va.

[10] Johnson, P. G., "The Utility of Nuclear Rockets in Inter-Orbit Transportation," ASME Space Technology and Heat Transfer Conference, Los Angeles, Calif., June 1970.

SEPTEMBER 1973 J. SPACECRAFT VOL. 10, NO. 9

Half- and Full-Model Experiments on Slender Cones at Angle of Attack

K. J. ORLIK-RÜCKEMANN,* J. G. LABERGE,† AND S. IYENGAR‡
National Aeronautical Establishment§, Ottawa, Ontario, Canada

An evaluation has been made of the angle-of-attack range at which experiments on slender sharp cones can be performed using half models. The evaluation was based partly on a comparison of surface flow patterns over full and half models, partly on the measurement of the static side force on full models at zero yaw, and partly on a comparison of oscillatory pitching results obtained with full and half models. Most of the results were obtained at a Mach number of two in the range of angle of attack between 0° and 30°, but the static side force was also measured at Mach numbers between 0.5 and 0.8. In all cases investigated it was found that up to an angle of attack of at least 15° no significant side force could be detected on full models, and that the pitch damping results and the surface flow patterns (with the exception of the primary attachment line) obtained on full and half models were in close agreement. The half-model technique appears therefore suitable for oscillatory experiments on slender cones (and probably on other similar geometries) at angles of attack at least up to 15°, at low supersonic speeds. Application to higher speeds, however, may very well require special corrections for tunnel-wall or reflection-plate boundary layer.

Nomenclature

C_m = (pitching moment)/(qSl)
$C_{m\theta} = \partial C_m/\partial\theta$, static pitching moment derivative
$C_{m\dot{\theta}} = \partial C_m/\partial(l\dot{\theta}/2V)$, pitch damping derivative
C_N = (normal force)/(qS)
$C_{N\theta} = \partial C_N/\partial\theta$
$C_{N\dot{\theta}} = \partial C_N/\partial(l\dot{\theta}/2V)$
C_Y = (side force)/(qS)
$k = \pi\nu l/V$, reduced frequency
l = model length
q = freestream dynamic pressure
S = base area of the model
V = freestream velocity
x_0 = distance of axis of oscillation from cone apex
α = (mean) angle of attack
$\theta, \dot{\theta}$ = angle of oscillation in pitch about a fixed axis, and its first derivative with respect to time
θ_c = cone semiangle
ν = oscillation frequency

Presented as Paper 72-1015 at the AIAA 7th Aerodynamic Testing Conference, Palo Alto, Calif., September 13–15, 1972; submitted September 25, 1972; revision received May 9, 1973.

Index category: Aircraft Testing (Including Component Wind Tunnel Testing).

* Head, Unsteady Aerodynamics Laboratory. Associate Fellow AIAA.

† Associate Research Officer.

‡ Research Associate; now Intermediate Engineer, Computing Devices of Canada.

§ A division of the National Research Council of Canada.

Introduction

FOR some wind-tunnel experiments the presence of a sting at the rear of a model may constitute a source of significant error. Alternative techniques to the conventional sting support are therefore of interest. One such technique involves the use of half models. Its application to oscillatory experiments at zero or low angles of attack (5°) was recently discussed by two of the present authors.[1,2] Since the interest in oscillatory experiments at higher angles of attack is rapidly increasing, an investigation was undertaken to determine the range of angle of attack in which this technique may be expected to give satisfactory results. Since any half-model technique can only be used when the flowfield is symmetric and similar to that on a corresponding full model, an examination of these aspects of the flow constituted an important part of the investigation. It consisted partly of measurements of the static side forces on full models at zero yaw and partly of a surface-flow visualization study on both full and half models. As a result, it was possible to determine the highest angle of attack at which the flow over a full, unyawed model still was symmetrical and at which the patterns of the flow-separation and flow-reattachment lines on full and half models still were in good agreement. The investigation was concluded with a series of oscillatory experiments using both full and half models, from which the static and dynamic pitching moment derivatives were determined. Most of the work was performed at a Mach number of 2 at angles of attack ranging from 0° to 30°, but the static side-force measurements were carried

out also at Mach numbers between 0.5 and 0.8. The NAE 30 in. × 15 in. trisonic suction wind tunnel was used for all experiments. Two slender cones, with semiangles of 7.75° and 10°, were used throughout the investigation.

Side-Force Measurements

The onset of unsymmetrical flow conditions on unyawed full models at an angle of attack was determined by side-force measurements, which were carried out using sting-supported models and a standard internal strain-gage balance. The sting was mounted an a variable incidence sector which for every Mach number was carefully adjusted in yaw for zero side force at zero angle of attack. The experiments were performed on full models of the two slender cones mentioned before and, in addition, on the full model of a sharp ogive-cylinder body with an ogive fineness ratio of 4.0 and a cylinder fineness ratio of 7.9. No boundary-layer trips were used in this part of the investigation. Since at subsonic speeds the flow asymmetry is known to occur at lower angles of attack than at supersonic speeds, the side-force measurements included several experiments at Mach numbers between 0.5 and 0.8, in addition to the main series of experiments at a Mach number of 2.

The results for the two cone models are shown in Figs. 1 and 2. At subsonic Mach numbers the side force became measurable at an angle of attack of about 15° for the 7.75° cone, and at 11°–12° for the 10° cone. At Mach 2 the corresponding figures were 21° for the 7.75° cone and 28° for the 10° cone, i.e., both resulting in a relative incidence, α/θ_c, of the order of 2.7–2.8. As is well-known, the direction of this side force depends on the initial asymmetry in the vortex shedding, which is triggered by some infinitesimal asymmetry or misalignment of the model; in the present experiments the side force happened to be in different directions for the two cone models.

The results for the ogive-cylinder are shown in Fig. 3. At subsonic Mach numbers the side force became measurable at an angle of attack of 16°–17°, but at Mach 2, apart from small deviations appearing locally at angles of attack between 15° and 21°, no fully developed asymmetry was observed in the entire range investigated, i.e., up to an angle of attack of 29°. In Fig. 3 the results obtained by Pick[3] at Mach 0.6, for a model of a similar shape and size, are shown for comparison. The Reynolds number of the two investigations was nearly the same and the results show a very good agreement.

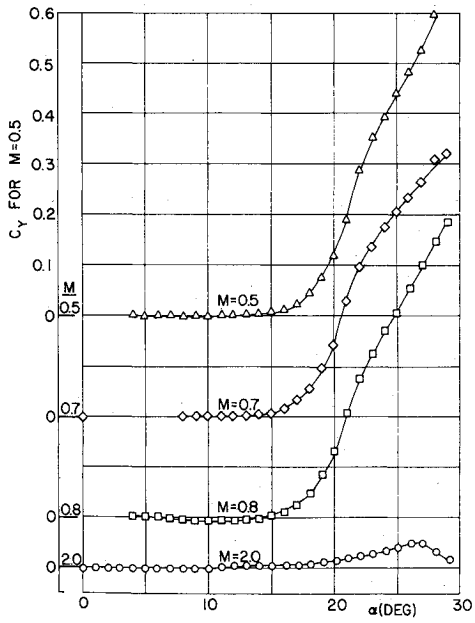

Fig. 1 Side force on unyawed 7.75° cone at angle of attack.

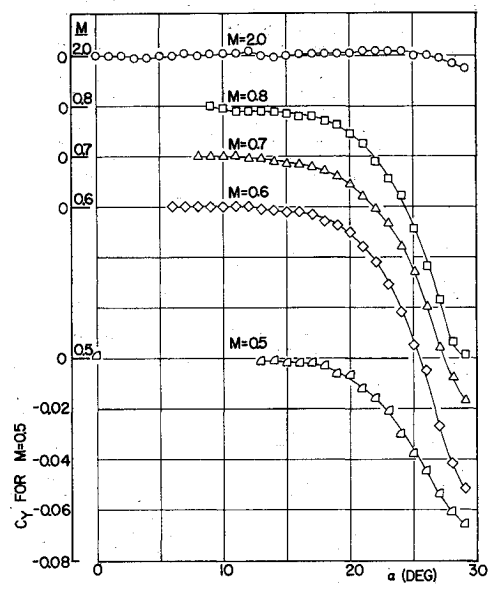

Fig. 2 Side force on unyawed 10° cone at angle of attack.

Surface-Flow Visualization

The separation and reattachment of the boundary layer on the leeward side of the 10° cone models at a Mach number of 2 was studied by means of a surface-flow visualization technique and the results for full and half models were compared. The half model, which was 8 in. long, was installed on a 12.25-in.-diam reflection plate that was mounted, by means of suitable supports, on the wind-tunnel wall at a distance of 0.75 in. from the wall (see Fig. 4), to ensure that the model is not affected by the wall boundary layer. A recessed well in the tunnel wall, of an area distribution similar to that of the reflection plate, served to reduce blockage effects. The supports consisted of a series of rotatable, wedge-shaped spacers with the main one in the center and five smaller ones distributed over the reflection plate in such a way as to keep its vibrations to a minimum. The supports were usually rotated such that the maximum misalignment of the wedges

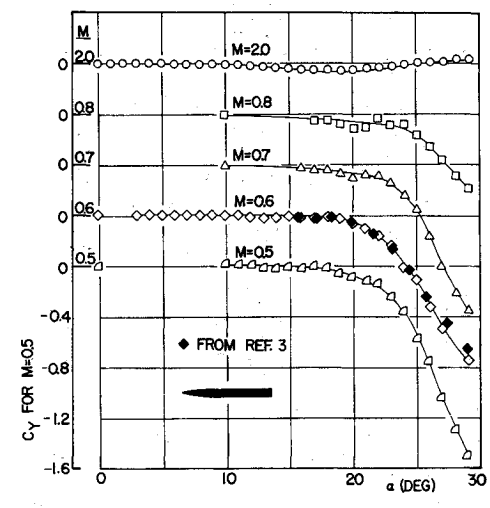

Fig. 3 Side force on ogive-cylinder at angle of attack.

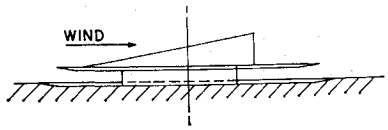

Fig. 4 Half model mounted on reflection plate.

with the flow was 5°. A 1 : 3 mixture of titanium oxide and vacuum pump oil together with a small quantity of oleic acid was used for flow visualization. Examples of the resulting photographs are shown in Figs. 5 and 6 (with the leeward meridian of the full model slightly rotated towards the camera to clarify the view). The meridian positions of the primary, and in some cases also of the secondary and the tertiary flow-separation lines, and of the corresponding flow-attachment lines, are plotted in Fig. 7 vs angle of attack. All cases discussed here involve the 10° cone with a boundary-layer trip, consisting of a 0.02-in.-thick flat nylon ring, located at about 0.5 in. from the apex of the cone. The corresponding results (not shown) obtained on the 10° cone without the trip were in most cases quite close to those shown, except for the secondary separation on the half model at angles of attack above 20°, where large effects of the trip were observed.

The flow visualization study indicated that: a) the primary attachment line on the half model at angles of attack up to 30° was displaced up to 27° from the windward meridian, due to the cross-flow pressure gradient caused by a lower pressure at the root of the half model; b) the meridian position of the primary separation line was nearly the same within 2°–3°, on both the full and the half model; c) the secondary attachment on the half model at angles of attack up to 20° was displaced by less than 6° from the leeward meridian and became rapidly more displaced at higher angles of attack; d) the meridian positions of the secondary separation line on the full model and on the half model were within 5° of each other up to an angle of attack of 20°; at higher angles of attack this difference increased with the separation line on the half

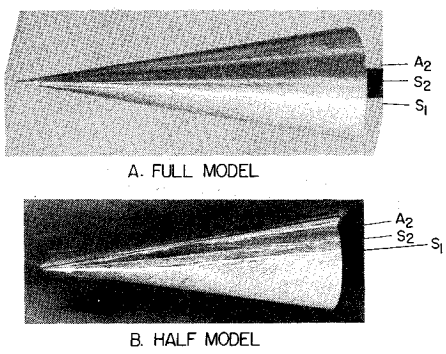

Fig. 5 Surface flow on 10° cone; $M = 2$; $\alpha = 15°$.

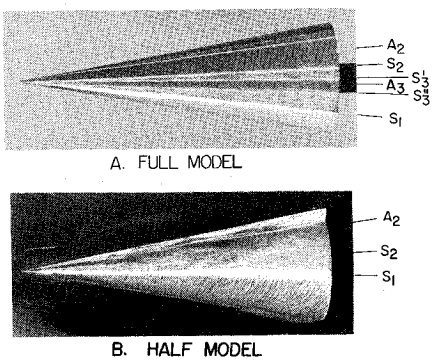

Fig. 6 Surface flow on 10° cone; $M = 2$, $\alpha = 30°$.

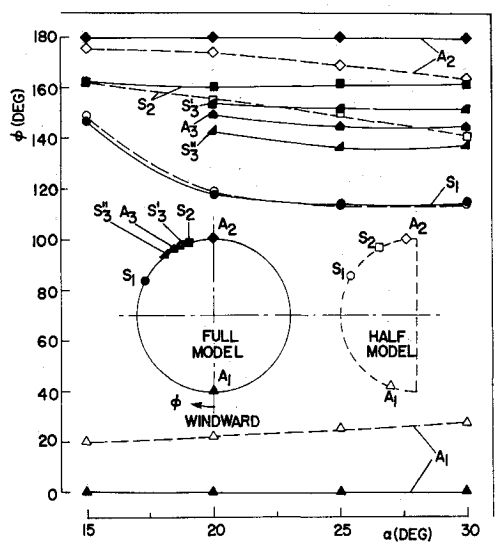

Fig. 7 Meridional position of flow-attachment (A) and flow-separation (S) lines on 10° cone; $M = 2$.

model moving further away from the leeward meridian; e) the tertiary attachment and separation could be observed only on the full model and only at angles of attack higher than 15°. It was also noted that at angles of attack of 10° and below, the primary attachment line was the only line that could be clearly distinguished on both models, and that at zero angle of attack even that line could no longer be seen on the half model.

Thus for angles of attack up to 20° the main difference between the surface flow pattern over the half model and the full model was the significant displacement of the primary attachment line from the windward meridian on the half model. However, the primary and secondary separation lines as well as the secondary attachment line showed a surprisingly good agreement. At angles of attack over 20° there were considerably more differences, although the primary separation still occurred at the same meridian.

Although obtained only at a Mach number of 2, these results are probably typical for low supersonic speeds. However, in view of the current interest in using the half-model technique also for hypersonic experiments, it should be noted, that the present results should not automatically be extended to hypersonic Mach numbers, where special experimental procedures and corrections may be required to account for the expected much larger effect of the reflection-plate boundary layer and its possible separation.

Oscillatory Pitching Experiments

The pitching experiments were performed using three different oscillatory techniques, namely 1) a half-model technique, 2) a full-model technique with external excitation, and 3) a full-model technique with internal excitation. Of these, the first two were initially developed for certain special applications and the third one was included as representative of the standard arrangement for this type of experiments. The results were obtained for both the 7.75° and the 10° cones and for models with and without the boundary-layer trip.

For experiments using the half-model technique (Fig. 8), a dynamic-test apparatus was mounted on the outside of the wind tunnel. The apparatus consisted of an elastic model suspension and an electromagnetic oscillator; for pitching oscillation the suspension was in the form of a cruciform spring to which the half model was firmly attached by means of an adaptor which passed right through both the wind-tunnel wall and the reflection plate. The oscillator consisted

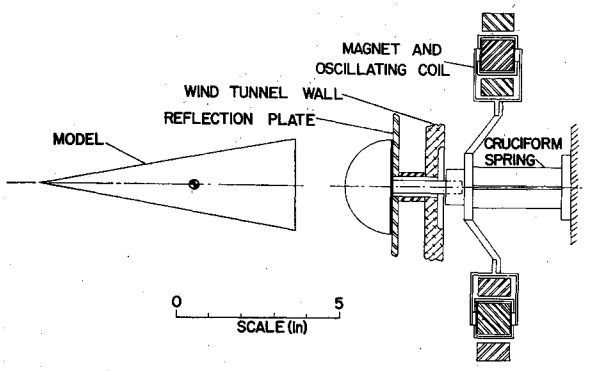

Fig. 8 Experimental arrangement for oscillation of half model.

of lightweight coils moving in a magnetic field and imparting a sinusoidal motion to the model end of the spring. Model position information was obtained from strain gages on the spring. More details are given in Refs. 1 and 2.

The arrangement for the full-model technique with external excitation consisted of a sting-mounted model, with the main stiffness of the oscillatory system provided by a pair of gimbal springs mounted outside the wind tunnel on the top and bottom walls, respectively, and attached to the model base by prestressed piano wires freely moving through a slot in the support sting. These wires were shielded from the flow by wedge-shaped wire guards. One of the springs was driven by an electromagnet, imparting an oscillatory motion to the model. The motion of the other spring was detected by a linear variable displacement transducer, with an output proportional to the model deflection. The sting deflection information was obtained from strain gages on the sting. More details can be found in Refs. 1 and 4.

The arrangement for the full-model technique with internal excitation (Fig. 9) consisted again of a sting-mounted model, but with the main stiffness of the oscillatory system provided by a cantilever spring inside the model and with the center of oscillation fixed by a flexural pivot attached to the sting. The rather unusual combination of these two features was made possible by the use of a flexible link for attaching the spring to the sting. The deflection and release of the model prior to the start of oscillation was produced by a solenoid-actuated spring-loaded tripper; several model releases could be made during a single wind-tunnel run. Model-position information was obtained from strain-gages on the spring and on the sting.

All three techniques made use of the free-oscillation method. For the full-model technique with external excitation and for the half-model technique, the standard NAE method of "free oscillation with automatically recycled feedback excitation" was used. For the full-model technique with internal excitation each model release was individually triggered. Standard calibration and data-reduction procedures were employed. The oscillation amplitude was 1.5° and the reduced frequency was in the range $0.041 < k < 0.069$. Run duration was of

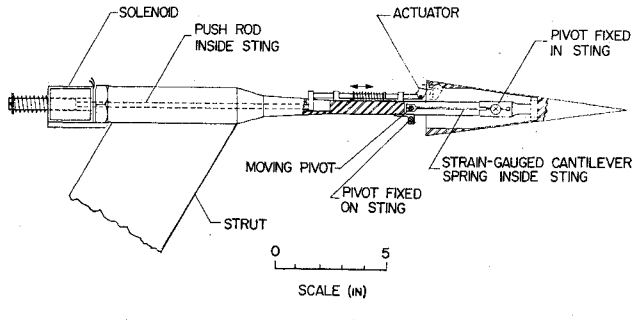

Fig. 9 Experimental arrangement for oscillation of full model with internal excitation.

the order of 13 to 14 sec allowing, on the average, three to four decays of model motion per run.

The static and dynamic results of the oscillatory experiments are presented in Figs. 10 to 14. To reduce the effect on the

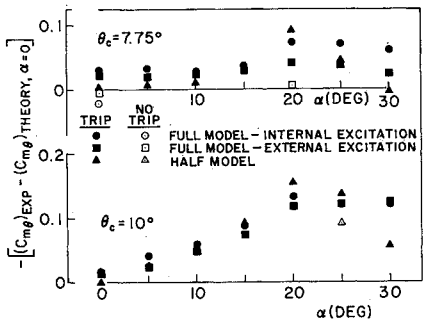

Fig. 10 Measured static pitching-moment derivative referred to theoretical value for cones at zero angle of attack.

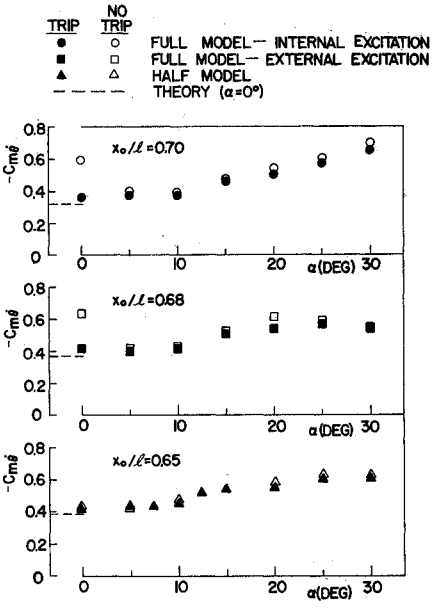

Fig. 11 Pitch damping for 7.75° cone; $M = 2$.

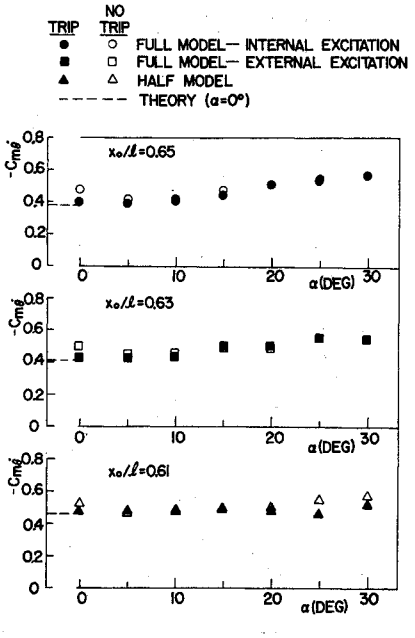

Fig. 12 Pitch damping for 10° cone; $M = 2$.

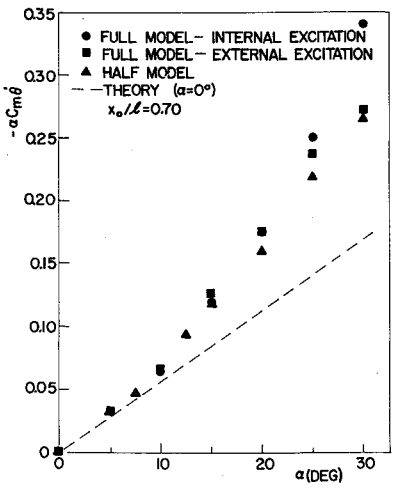

Fig. 13 Normalized pitch damping for 7.75° cone with trip; $M = 2$.

results of the position of axis of oscillation, x_0/l (which varied slightly during the various parts of the experiments), the static pitching moment derivative, $C_{m\theta}$, is given in Fig. 10 as the difference between the value measured and that obtained theoretically, from Ref. 5, for zero angle of attack. For clarity, Fig. 10 shows mainly the results for models with the boundary-layer trip; for models without the trip only those results are included, that significantly differ from those for models with the trip. In general the agreement is fairly good up to an angle of attack of 15°, although the half-model results—especially for the 7.75° cone—tend to be somewhat lower than the corresponding full-model results. This is attributed to the well-known[6] effect of the loss of lift caused by the necessary small gap between the half model and the reflection plate. The effect is concentrated on the part of the half model in the vicinity of the gap (as also indicated by the meridional displacement of the primary attachment line on the half model) and its importance on the total lift (or pitching moment) diminishes when the lateral dimensions of the model become large as compared to the width of the gap.

The variation of the pitch-damping derivative, $-C_{m\dot{\theta}}$, with angle of attack is illustrated in Figs. 11 and 12. In the presence of the boundary-layer trip the damping on both the full and the half models remained fairly constant up to an angle of attack of about 10°. This plateau was usually slightly higher than the prediction of zero angle-of-attack supersonic potential theory.[5] At higher angle of attack, damping in the standard internal excitation case increased almost linearly with α. This is in very good agreement with both experimental and theoretical results recently published.[7] The rate of increase with α was smaller for the 10° cone than for the 7.75° cone. The full model with external excitation and the half model also displayed an increase in damping at angles of attack higher than 10°, but the increase was not linear. For the half-model data for the 10° cone this variation was quite flat but irregular. The half-model data for the 7.75° cone at $\alpha = 10°$ displayed an unusually large amount of scatter.

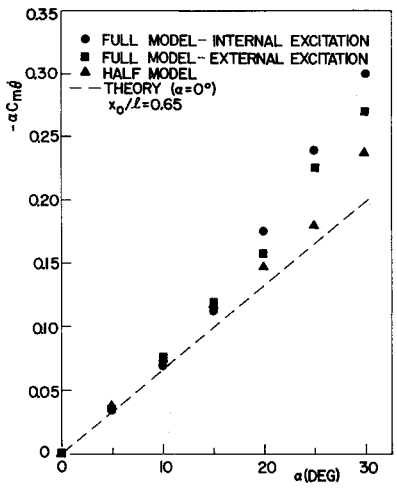

Fig. 14 Normalized pitch damping for 10° cone with trip; $M = 2$.

In all cases the absence of the boundary-layer trip resulted in a local increase in damping at zero angle of attack. This increase was more pronounced for the 7.75° cone than for the 10° cone and was much larger for the full model than for the half models. Although no full explanation of this phenomenon can be offered at present, it is possible that it may be related to a dynamic sting-interference effect[8] which sometimes, in the presence of boundary-layer transition near the cone base, may cause the transition to move upstream from the base area. Although no experiments were undertaken to determine whether the transition actually occurred near the base, this possibility was strongly indicated, especially for the 7.75° cone, by the magnitude of the local Reynolds number, based on the cone length. This explanation was also supported by additional experiment (not reported herein) at a much higher reduced frequency ($k = 0.15$), that produced larger sting oscillation and resulted in an even higher zero angle-of-attack value of the $(-C_{m\dot{\theta}})$ derivative for the 7.75° cone without the trip. The presence of such a transition-induced support interference on full models with no trip at zero angle of attack was further supported by the fact, that for these conditions the static stability derivative, $-C_{m\theta}$, was considerably lower (Fig. 10) than for full models with the trip, in accordance with Ref. 8, which predicts opposite effects of sting-support interference on static and dynamic stability.

For an easier comparison of the pitch-damping results of the various parts of the experiments, all damping results were normalized with respect to the axis position for the full model with internal excitation. The normalization was carried out using the following axis-transfer equation:

$$C_{m\dot{\theta}_2} = C_{m\dot{\theta}_1} - (x/l)C_{N\dot{\theta}_2} + (2x/l)C_{m\theta_1}\cos\alpha - 2(x/l)^2 C_{N\theta}\cos\alpha + 4(x/l)\,C_{m_1}\sin\alpha - 4(x/l)^2 C_N \sin\alpha$$

where subscript "1" refers to the aft axis and subscript "2" to the parallel forward axis at a distance x upstream. Since the derivatives on the right-hand side were based on zero angle-of-attack theory, the normalization was valid, in a strict sense, only for low angles of attack. However, for the sake of uniformity, it was applied to the entire range of angles of attack covered by the experiments.

The normalized values of $(-\alpha C_{m\dot{\theta}})$ are shown in Figs. 13 and 14. To avoid irregularities caused by the dynamic sting interference on the boundary-layer transition, only data obtained with the boundary-layer trip were considered. For both cones the agreement between the three methods was very good up to $\alpha = 15°$. At higher angles of attack the results obtained with the full model with external excitation and with the half model were generally lower than those obtained with the full model with internal excitation. In the case of the external excitation, this was probably due to the interference of the wire guards on the flow near the base of the model. In the case of the half model, the differences were probably caused by the boundary layer on the reflection plate and by the gap between the model and the plate, which obviously affected the position of the flow separation lines and vortices on the leeward side of the model.

Conclusions

On the basis of comparative full-model and half-model oscillatory experiments, surface-flow studies and side-force measurements on two slender cones at a Mach number of 2 and an angle of attack up to 30°, the following conclusions may be reached: a) surface-flow patterns on the half-model resemble closely those on the full model up to an angle of attack of 20°, except for a significant displacement of the

primary attachment line from the windward meridian on the half model; b) no significant side forces are present on the full model at zero yaw up to an angle of attack of 20° (however, at subsonic speeds a measurable side force has been observed at an angle of attack of 11°); and c) pitch-damping results obtained with a half-model technique and with two full-model techniques are in very good agreement up to an angle of attack of 15°.

It should be noted that the displacement of the primary attachment line on the half model, although obviously of little importance for the damping results, has a more pronounced effect on the static aerodynamic coefficients. That notwithstanding, the present investigation confirms the suitability of the half-model oscillatory technique for determining supersonic pitch damping on pointed slender bodies at an angle of attack of up to 15°.

References

[1] Orlik-Rückemann, K. J., Adams, P. A., and LaBerge, J. G., "Dynamic Stability Testing of Unconventional Configurations," *Journal of Aircraft*, Vol. 9, No. 2, Feb. 1972, pp. 101–102.

[2] Orlik-Rückemann, K. J., LaBerge, J. G., and Hanff, E. S., "Supersonic Dynamic Stability Experiments on the Space Shuttle," *Journal of Spacecraft and Rockets*, Vol. 9, No. 9, Sept. 1972, pp. 655–660.

[3] Pick, G. S., "Side Forces on Ogive-Cylinder Bodies at High Angles of Attack in the $M = 0.5$ to 1.1 Range," AIAA Paper 71–570, Palo Alto, Calif., 1971.

[4] Orlik-Rückemann, K. J., LaBerge, J. G., Adams, P. A., and Conlin, L. T., "A Wind-Tunnel Apparatus for Dynamic Stability Experiments on Sting-Mounted Slender Bodies," LTR-UA-13, March 1970, National Research Council of Canada, Ottawa, Canada.

[5] Tobak, M. and Wehrend, W. R., "Stability Derivatives of Cones at Supersonic Speeds," TN 3788, 1956, NACA.

[6] Orlik-Rückemann, K. J. and LaBerge, J. G., "Static and Dynamic Longitudinal Stability Characteristics of a Series of Delta and Sweptback Wings at Supersonic Speeds," Aero. Rept. LR-396, Jan. 1966, National Research Council of Canada, Ottawa, Canada.

[7] Stone, G. W., Clark, E. L., Jr., and Burt, C. E., "An Investigation of Nonsymmetrical Aerodynamic Damping Moments," AIAA Paper 72–29, San Diego, Calif., 1972.

[8] Ericsson, L. E. and Reding, J. P., "Boundary-Layer Transition and Dynamic Sting Interference," *AIAA Journal*, Vol. 8, No. 10, Oct. 1970, pp. 1886–1888.